Hybrid Nanogenerator for Concurrently Harvesting Biomechanical and Biochemical Energy

Benjamin J. Hansen,[†] Ying Liu,[†] Rusen Yang, and Zhong Lin Wang*

School of Material Science and Engineering, Georgia Institute of Technology, Atlanta, Georgia 30332. [†]These authors contributed equally.

ARTICLE

ABSTRACT Harvesting energy from multiple sources available in our personal and daily environments is highly desirable, not only for powering personal electronics, but also for future implantable sensor-transmitter devices for biomedical and healthcare applications. Here we present a hybrid energy scavenging device for potential *in vivo* applications. The hybrid device consists of a piezoelectric poly(vinylidene fluoride) nanofiber nanogenerator for harvesting mechanical energy, such as from breathing or from the beat of a heart, and a flexible enzymatic biofuel cell for harvesting the biochemical (glucose/O_2) energy in biofluid, which are two types of energy available *in vivo*. The two energy harvesting approaches can work simultaneously or individually, thereby boosting output and lifetime. Using the hybrid device, we demonstrate a "self-powered" nanosystem by powering a ZnO nanowire UV light sensor.

KEYWORDS: hybrid cell · piezoelectric · PVDF · electrospinning · nanogenerator · biofuel cell · energy harvesting

The ever increasing energy demand of modern society is perhaps among the greatest challenges humankind is and will continue to face. Research in energy includes but is not limited to the following major areas: mega-scale energy conversion, renewable and green energy, efficient energy transmission, energy storage, energy harvesting, and sustainable power source for micro- or nanosystems. In addition to large-scale energy harvesting from "renewable" sources, such as wind, hydro, and solar, there is also significant opportunity to harvest the wasted energy in our personal environments, such as from walking, typing, speaking, and breathing. If efficiently harvested to its full potential, many of the modern energy requirements needed for small devices and even personal electronics could be fulfilled. This is a new trend in the worldwide effort in developing technologies related to energy scavenging.[1−3]

Energy harvested from the environment will likely be sufficient for powering nanodevices used for periodic operation, owing to their extremely low power consumption and small sizes. For example, an implantable device that wirelessly communicates the local glucose concentration for diabetes management, the local temperature for infection monitoring after surgery, or a pressure difference to indicate blockage of fluid flow in the central nervous system and blood clotting can all be foreseen as potential applications that need implantable energy sources. Powering such devices could be accomplished by concurrently harvesting energy from multiple sources within the human body, including mechanical and biochemical energy to augment or even replace batteries. However, powering implantable nanodevices for biosensing using energy scavenging/harvesting technology is rather challenging because the only available energy *in vivo* is mechanical, biochemical, and possibly electromagnetic energy, whereas thermal energy cannot be harvested due to lack of an adequate temperature gradient, and solar energy is not available for devices implanted inside the body.

A recent breakthrough in harvesting mechanical energy by nanowire based nanogenerators (NG) has demonstrated an excellent route for harvesting the biomechanical energy created from tiny physical motion, such as the inhaling/exhaling of lungs or the beat of a heart.[4−8] In addition, approaches have been demonstrated for converting the biochemical energy of glucose/O_2 in biofluid using active enzymes as catalysts in a compartmentless biofuel cell (BFC).[9−11] In this paper, we demonstrate the first integrated operation of a hybrid nanogenerator composed of a nanogenerator and biofuel cell for simultaneously or independently harvesting mechanical and biochemical energy, with the aim of building

*Address correspondence to zlwang@gatech.edu.

Received for review April 21, 2010 and accepted May 24, 2010.

Published online May 27, 2010.
10.1021/nn100845b

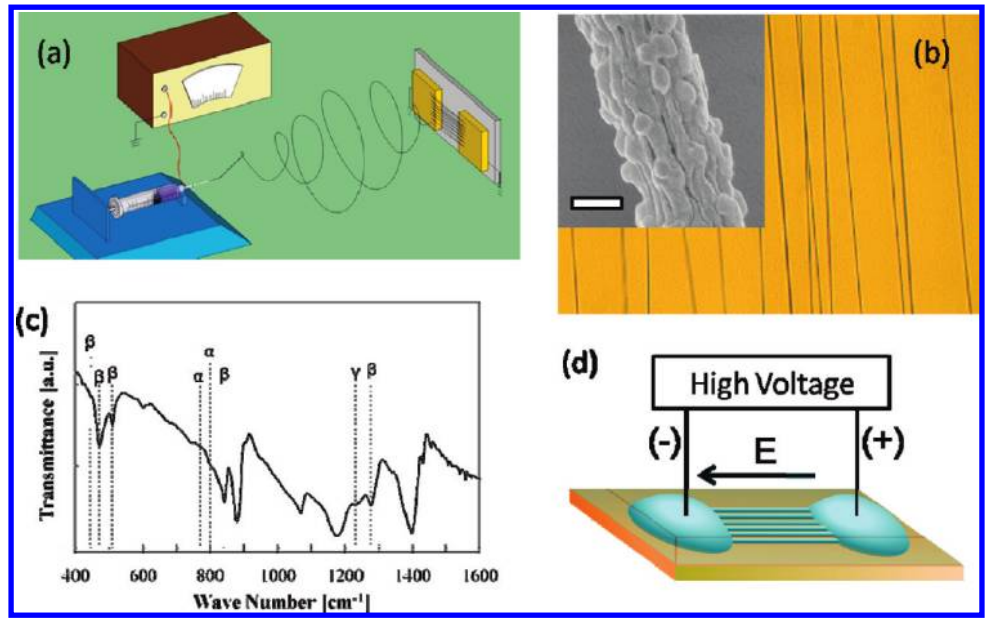

Figure 1. (a) Schematic of the electrospinning process to obtain aligned PVDF NFs. (b) Optical image of aligned PVDF NFs on Kapton film and high resolution SEM of NF surface morphology shown in the inset (400 nm). (c) FTIR transmission spectrum of PVDF NFs. (d) Schematic of the high field in-plane poling of PVDF NFs.

self-powered nanodevices/nanosystems for *in vivo* biomedical and other applications where the two types of energy are available, such as living plants. We have also used the hybrid nanogenerator to drive a single nanowire-based UV nanosensor to demonstrate the possibility of a "self-powered" nanosystem.

RESULTS AND DISCUSSION

Harvesting Mechanical Energy by Nanogenerator. The NG based on a single ZnO nanowire that is laterally bonded onto a polymer substrate was first demonstrated by our group.[5] Based on a similar mechanism and design, a NG using a single piezoelectric poly(vinylidene fluoride) (PVDF) nanofiber (NF) was reported recently.[12] In our hybrid design we use PVDF nanofibers as the working component for the mechanical energy harvester. Cheng *et al.* used near-field electrospinning to synthesize the single PVDF NFs, where the high electric field used to draw the NF was suggested to naturally align the dipoles along the NF long axis. Alternatively, we used conventional electrospinning (see Experimental Methods for details) with the two electrode technique[13] to synthesize and pattern an array of aligned NFs, followed by a post, in-plane poling process (Figure 1a−d). A scanning electron microscopy (SEM) image (Figure 1b, inset) reveals the textured morphology on the NF surface, presumably resulting from the formation of small crystallites. Fourier transform infrared spectroscopy (FTIR) was used to characterize the crystal phases present in the PVDF NFs. The FTIR transmission spectrum of the as-spun PVDF nanofibers is presented in Figure 3c. A mixture of the polar β phase and the nonpolar α and γ phases was indexed.[14] The random dipole orientation of the polar β phase was oriented by encasing the device in PDMS and performing high-field (~0.2 MV/cm) in-plane poling (Figure 1d) for ~15 min (see Experimental Methods for details).

The working principle of the PVDF NG is based on the insulating property of the PVDF NF and the creation of an inner piezoelectric field during applied tensile strain.[5,12] As the device is deformed under alternating compressive and tensile force (Figure 2c,d), the NF acts like a "capacitor" and "charge pump", which drives a flow of electrons back and forth through the external circuit. This charging and discharging process results in an a.c. power source.

The strain rate dependence on the open-loop voltage and short-circuit current produced by a PVDF NG undergoing cyclic mechanical loading is presented in Figure 2a,b. The induced strain was fixed at ~0.05% and applied over 0.06, 0.04, and 0.03 s. By increasing the strain rate over this range, the open loop voltage increased from 15 to 20 mV and the short circuit current increased from 0.2 to 0.3 nA, which is consistent with piezoelectric theory.[15] The output voltage is dictated by individual nanowire, while the output current is the sum of those from all of the active nanowires. The output of the PVDF NG could be improved by replacing PDMS with a material having a higher breakdown voltage, so that higher poling fields could be applied to obtain a greater remnant polarization.[16,17] In addition, hundreds of NFs could potentially be integrated together and connected in series and/or parallel to further improve the power output.[7]

Harvesting Biochemical Energy by Biofuel Cell. An enzymatic BFC was used to convert the chemical energy of glucose and oxygen in biofluid into electricity. The BFC configuration used in this study is illustrated in Figure

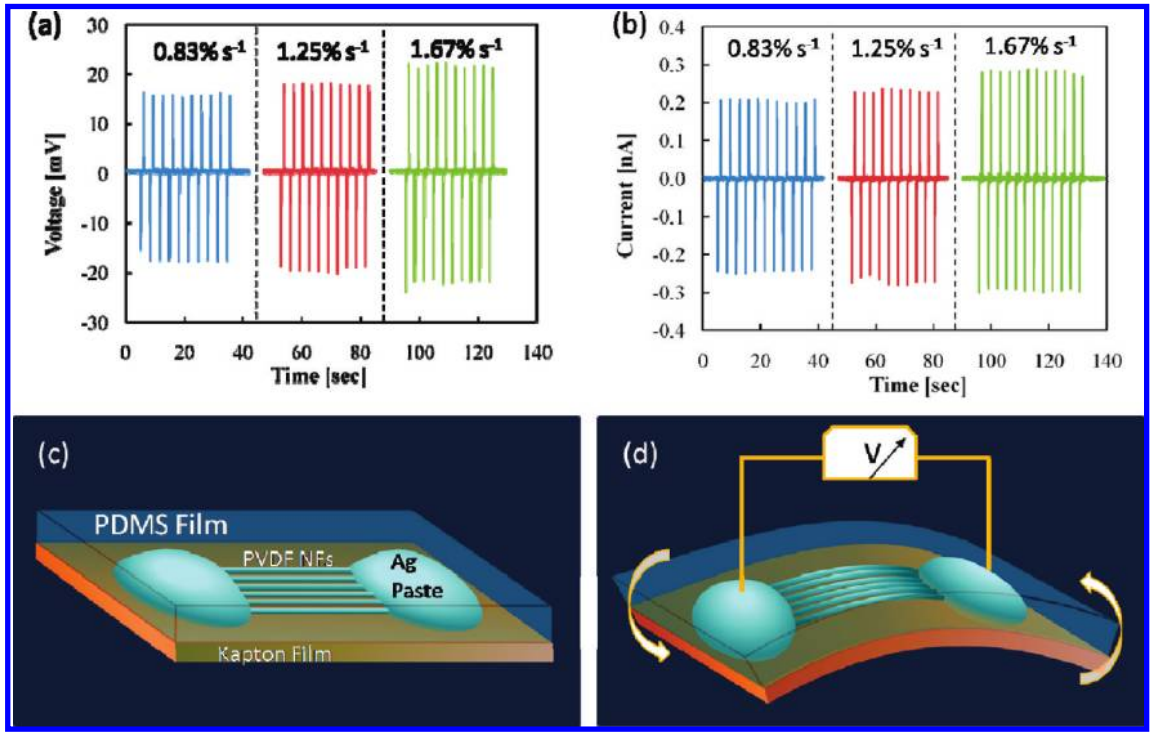

Figure 2. Open-loop voltage (a) and short-circuit current of a PVDF NG as a function of strain rate with a maximum strain of ~0.05%. (c) The PVDF NF lies on a Kapton substrate, with both ends bonded with silver paste and the entire device encapsulated with PDMS. (d) Mechanical bending of the substrate creates tensile strain and a corresponding piezoelectric field along the fiber that drives the electrons through an external load back and forth following the cycled mechanical action.

3c. The electrodes were patterned onto Kapton film and coated with multiwall carbon nanotubes (MWCNTs), followed by immobilization of glucose oxidase (GOx) and laccase to form the anode and cathode, respectively (see Experimental Methods for details). In addition to immobilizing the enzymes onto the electrodes, it has been shown that CNTs help promote the electron transfer between the enzymes and the electrodes.[18−20] The operating principle of the BFC is illustrated in Figure 3d. When the device is in contact with a biofluid that contains glucose (such as blood), the corresponding chemical processes occurring at the

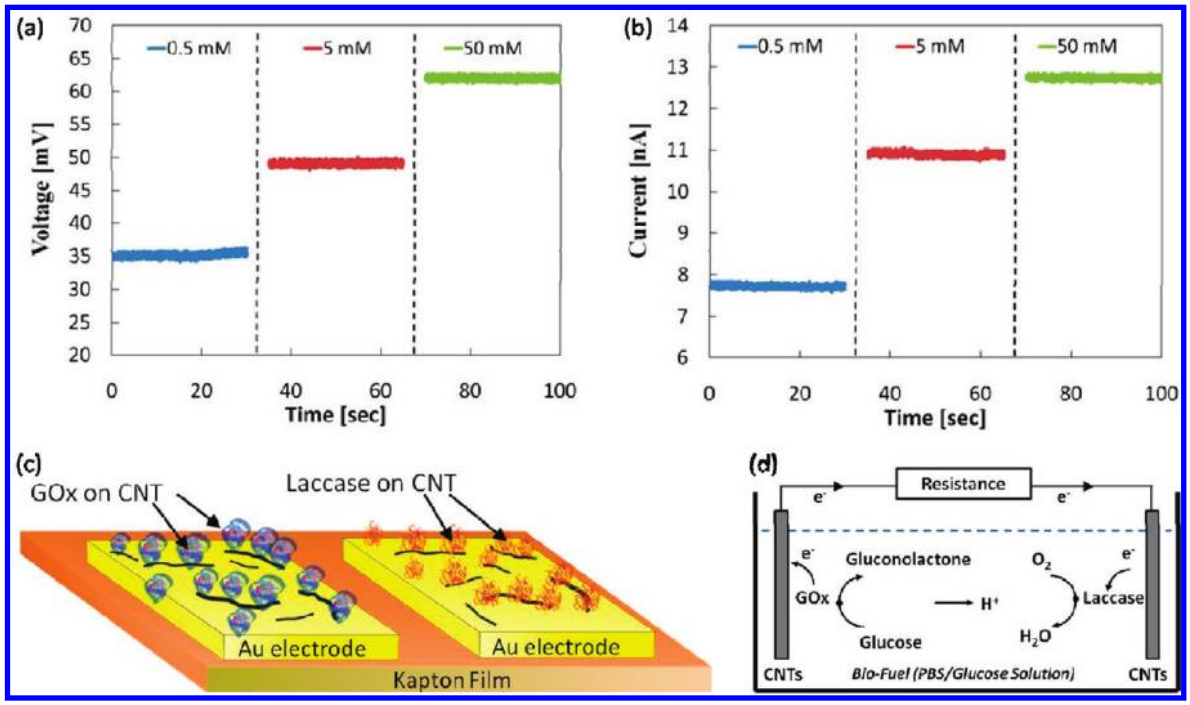

Figure 3. Open-loop voltage (a) and short-circuit current (b) of the BFC as a function of glucose concentration in PBS solution. (c) Schematic illustration of the fabricated BFC device. (d) Simplified schematic of the BFC operating mechanism.

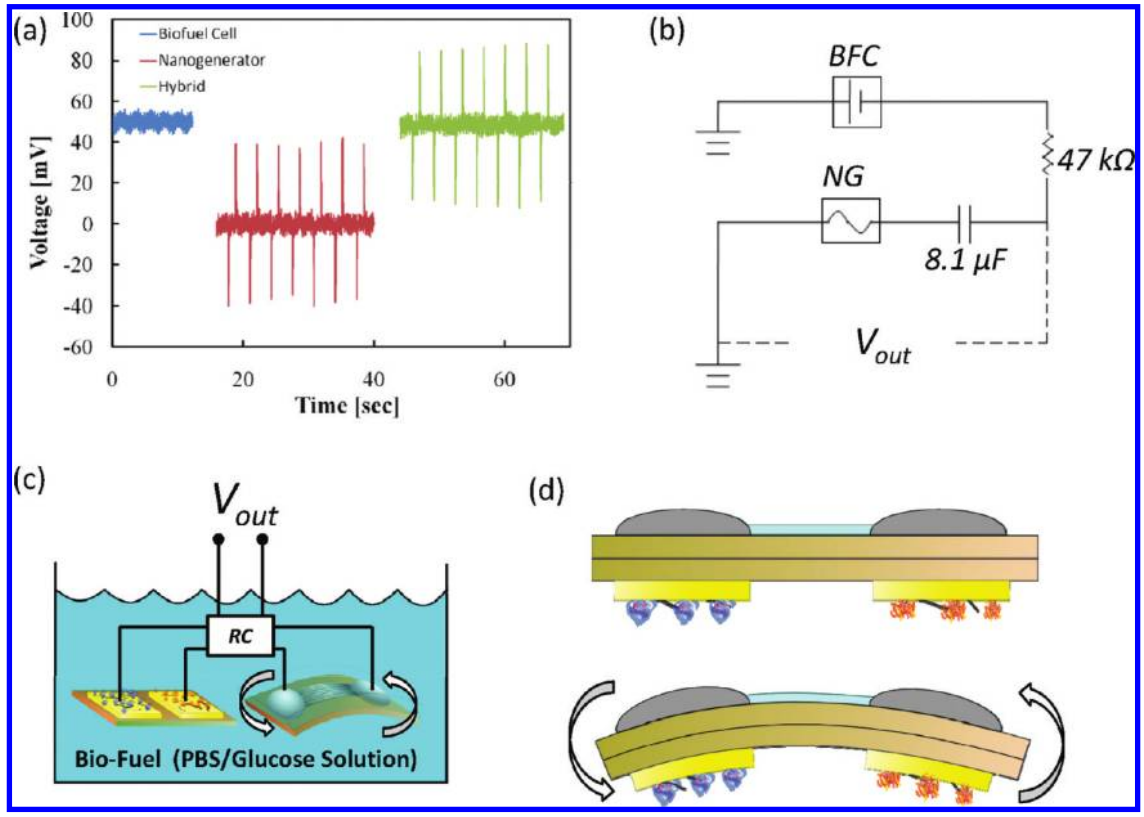

Figure 4. (a) Open-loop voltage of the independent and combined operation of the BFC and PVDF NG. (b) Circuit diagram used for integration of the hybrid BFC-NG device. Note, with considering the inner resistance of the NG, the time required to charge the capacitor is much longer than the period at which the strain was applied to the NG, so that the output *V* is a sum of those from BFC and NG. (c) Schematic of hybrid device integration. (d) Conceptual design of a BFC-NG hybrid device.

two electrodes is:[9] glucose is electro-oxidized to gluconolactone at the anode, $\text{glucose} \xrightarrow{\text{GOx}} \text{gluconolactone} + 2H^+ + H_2O$, and dissolved O_2 is electro-reduced to water at the cathode, $1/2O_2 + 2H^+ + 2e^- \xrightarrow{\text{laccase}} H_2O$.

The open-loop voltage and short-circuit current produced by the BFC operating in phosphate buffer solution (PBS, pH 7.0) with glucose concentrations of 0.5, 5, and 50 mM is presented in Figure 3a,b. Both the current and the voltage were found to increase with increasing glucose concentration. Human blood has a glucose concentration that fluctuates between ~4 and 6 mM and has a pH of 7.35−7.45.[9] At 5 mM, the open loop voltage was found to be 50 mV and a short-circuit current of 11 nA. The power density of the BFC depends on load matching and was found to have a maximum at ~10 MΩ with a corresponding power density of ~2.2 nW/cm^2 and a current density of ~58 nA/cm^2 (see Supporting Information).

The highest theoretical voltage that may be obtained from a GOx/laccase-based BFC is dictated by thermodynamics and is ~1 V.[9] To obtain this voltage, various factors need to be optimized, but the most important one is the enzyme surface interactions. By cross-linking or "wiring" the immobilized redox enzymes to a redox hydrogel, the output of the BFC can be further optimized in the future.[21−23] In addition, multiple BFCs could be integrated together to boost power output.

Hybrid Biochemical and Biomechanical Nanogenerator. One of the major hurdles of a glucose/O_2 BFC is the performance degradation over time due to the decay of the living enzymes.[11,20] Therefore, a hybrid BFC-NG, which concurrently harvests mechanical and biochemical energy, is highly attractive for its increased power output and lifetime. The BFC has the benefit of high power density, whereas the PVDF NG has the benefit of potentially operating over much longer times because the lifetime is only limited by the mechanical fatigue of the device and can eventually be engineered to last.

The independent and integrated operation of the PVDF NG, the BFC, and the hybrid BFC-NG is presented in Figure 4a−c. To integrate the AC voltage of the PVDF NG with the DC voltage of the BFC, a simple RC high pass filter (Figure 4b) was used, which effectively blocks the DC voltage of the BFC in one direction while passing the AC voltage of the NG. By integrating the two devices, the peak voltage was nearly doubled from ~50 to ~95 mV. Furthermore, the PDMS packaging of the PVDF NG allows for operation inside biofluid and *in vivo* environments. In addition, using a flexible Kapton film substrate for the BFC permits the devices to be

integrated back-to-back as conceptually illustrated in Figure 4d. It is important to point out that our goal here is not to maximize the output of BFC; instead, we keep the output of the BFC to be in a reasonable range so that the hybridization of the BFC and NG can be clearly illustrated.

The power output of the hybrid nanogenerator is the sum of the BFC and NG. The voltage output of the BFC is V_{BFC}, and the output voltage of the ac NG is $\pm V_{NG}$. Considering the infinitely large resistance of the PVDF nanofiber, the output voltage of the NG component is $\pm V_{NG}$, even with the presence of a load. The inner resistance of the BFC is rather low because it is dictated by electron transfer between the active center of the enzymes and the CNT electrodes. In such a case, the voltage applied to an external load R is $V_{BFC} \pm V_{NG}$, which gives an output power of $(V_{BFC} \pm V_{NG})^2/R$. The average peak output power for each cycle of the mechanical action is $[(V_{BFC} + V_{NG})^2/R + (V_{BFC} - V_{NG})^2/R]/2 = (V_{BFC})^2/R + (V_{NG})^2/R$. In addition, methods can eventually be developed for rectification of the a.c. NG output to obtain a d.c. signal and integration with the d.c. output of the BFC to give an overall enhanced d.c. output.

Powering Nanosensor by Hybrid Cell. The hybrid BFC-NG was also used to drive the operation of a ZnO nanowire-based UV light sensor (Figure 5b). When there was no UV light, the resistance of the ZnO nanowire was ~7 MΩ (see Supporting Information), and the corresponding peak voltage drop on the nanosensor was ~5 mV, as shown in Figure 5a. Upon irradiation with UV light, the nanowire resistance dropped to ~800 kΩ and the peak voltage drop across the nanowire device was reduced to ~2.5 mV. This demonstrates the potential of a fully "self-powered" nanosystem for *in vivo* applications.

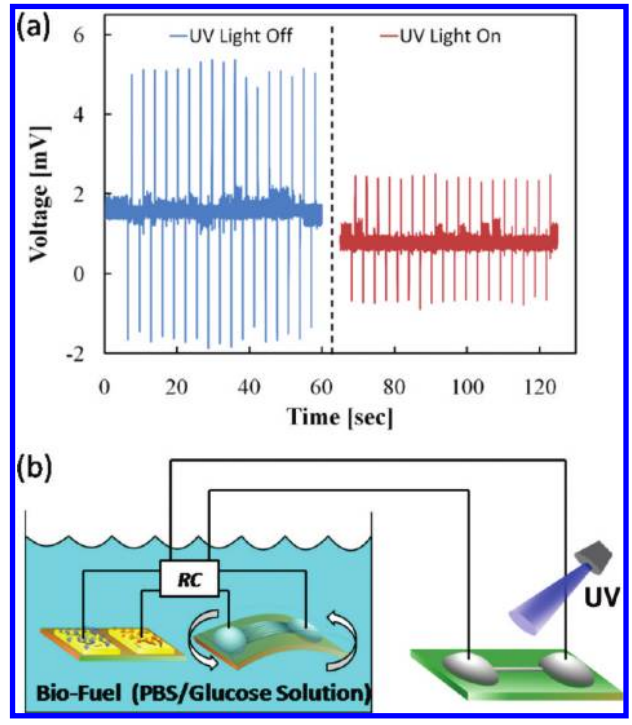

Figure 5. Integration of the hybrid BFC-NG device with a UV nanosensor to demonstrate a "self-powered" nanosystem. (a) Voltage drop across the ZnO NW UV light sensor when the UV light is off and on. For illustration purposes, only stabilized signals are displayed. (b) Schematic illustration of the self-powered hybrid nanosystem.

CONCLUSION

Developing energy scavenging technology that harvests multiple-type energy sources from our personal environments is highly desired for sustainable energy production and unique applications. Previously, we have demonstrated the first hybrid cell for simultaneously harvesting solar and mechanical energy.[24] Here, we have demonstrated a hybrid device that can be used to simultaneously scavenge both biochemical and mechanical energy for *in vivo* applications. The hybrid device takes advantage of its two constituent parts, leading to a higher output and potentially longer operating lifetimes. In addition, the hybrid device was used to power a UV nanosensor, demonstrating the outstanding potential for a completely self-powered nanosystem for *in vivo* biomedical applications.

EXPERIMENTAL METHODS

Electrospinning of PVDF Nanofibers. PVDF powder (MW 534000) was purchased from Sigma-Aldrich and used as received. A total of 1.5 g PVDF was dissolved in a mixture of 3 mL of DMF (VWR) and 7 mL of acetone (VWR) and heated at 60 °C for 30 min so that the solution was homogeneous. The transparent viscous solution was transferred into a Hamilton 1 mL syringe for electrospinning. A Chemyx Fusion 200 syringe pump and Betran DC High Voltage power supply were used, a voltage of 12 kV was applied to the syringe needle, and a feed rate of 50 μL/min was used. The electrospun fibers were collected onto two grounded copper pieces with a 2 cm gap, placed 15 cm away from the needle, and the fibers were electrostatically aligned across the electrode gap.

Fabrication and In-Plane Poling of Nanogenerator. A 1 cm × 2 cm × 30 μm Kapton@Dupont thin film was used as the supporting substrate. To form two electrodes a 50 nm thick layer of Au was deposited onto the Kapton substrate, leaving a 1 mm uncoated gap in the middle by using a mask. The electrospun fibers were carefully transferred across the Au electrodes and electrically bonded using silver paint (Ted Pella). A 0.5 mm layer of PDMS was deposited over the device for dielectric protection and biocompatibility. The final device was immersed into paraffin oil and 20 kV was applied between the two electrodes for 15 min. After poling, the electrodes were shorted for over 12 h.

Biofuel Cell Fabrication. Glucose oxidase (GOx, from *Aspergillus niger*, type X-S) and laccase powder (from Trametes versicolor) were purchased from Sigma-Aldrich, multiwall carbon nanotubes from Hanhwa Nanotech (diameter 3−9 nm, purity >95%), and phosphate buffer solution (PBS, pH 7.0) from Fluka. All chemicals were used as received. Carbon nanotubes were dissolved in ethanol and sonicated for 1 h to form 2 g/L dispersion. A 4 g/L solution of GOx in phosphate buffer solution and a 4 g/L solution of laccase in phosphate buffer solution was prepared. The Kapton film with Au electrodes was prepared as described and then bleached and rinsed with deionized water

before use. A total of 2 μL of CNT dispersion was deposited onto both electrodes and rinsed with deionized water after drying. GOx solution (2 μL) was then deposited onto one of the CNT/Au electrodes to form the anode and 2 μL of laccase solution was deposited onto the other to form the cathode. The device was then stored under 4 °C for at least 4 h before use. Prior to use, the electrodes were rinsed in pure PBS.

Electrical Measurement. A voltage preamplifier (Stanford Research Systems, Model SR560) and a current preamplifier (Stanford Research Systems, Model SR560) were used to measure voltage and current output of the devices, respectively. A labview program was used to monitor and record the measurement. A DC linear motor was used to provide strain for the nanogenerator measurement.

FTIR and SEM Imaging. A Nicolet Magna IR 560 spectrometer was used to obtain the FTIR transmission spectrum of a 1 mm thick layer of PVDF nanofibers. Prior to SEM imaging, PVDF nanofibers were deposited onto silicon substrate and coated with a thin (~5 nm) layer of Au. The surface morphology of the PVDF nanofibers was analyzed using a LEO 1530 SEM at 5 kV accelerating voltage.

Acknowledgment. Research was supported by DARPA (Army/AMCOM/REDSTONE AR, W31P4Q-08-1-0009), BES DOE (DE-FG02-07ER46394), KAUST Global Research Partnership, NSF (DMS0706436, CMMI 0403671), MANA WPI program from NIMS, Japan, and the Georgia Institute of Technology. B.J.H. was supported by a National Science Foundation Graduate Research Fellowship. We thank Prof. Jing Zhu and Dr. Caofeng Pan for technical discussions. Thanks to Yagang Yao and Ziyin Lin for FTIR work and Hao Fang for Au deposition.

Supporting Information Available: Power, voltage, and current characteristics of the BFC, voltage output of the PVDF NG as a function of load resistance, hybrid BFC-NG with different strain rates, PVDF NG current and voltage polarity reversal tests, and ZnO nanowire UV sensor *I*−*V* curves. This material is available free of charge via the Internet at http://pubs.acs.org.

REFERENCES AND NOTES

1. Wang, Z. L. Towards Self-Powered Nanosystems: From Nanogenerators to Nanopiezotronics. *Adv. Funct. Mater.* **2008**, *18*, 3553–3567.
2. Priya, S. Advances in Energy Harvesting Using Low Profile Piezoelectric Transducers. *J. Electroceram.* **2007**, *19*, 165–182.
3. Pan, C.; Wu, H.; Wang, C.; Wang, B.; Zhang, L.; Cheng, Z.; Hu, P.; Pan, W.; Zhou, Z.; Yang, X.; Zhu, J. Nanowire-Based High-Performance "Micro Fuel Cells": One Nanowire, One Fuel Cell. *Adv. Mater.* **2008**, *20*, 1644–1648.
4. Wang, Z. L.; Song, J. H. Piezoelectric Nanogenerators Based on Zinc Oxide Nanowire Arrays. *Science* **2006**, *312*, 242–245.
5. Yang, R. S.; Qin, Y.; Dai, L.; Wang, Z. L. Power Generation with Laterally Packaged Piezoelectric Fine Wires. *Nat. Nanotechnol.* **2009**, *4*, 34–39.
6. Yang, R. S.; Qin, Y.; Li, C.; Zhu, G.; Wang, Z. L. Converting Biomechanical Energy into Electricity by a Muscle-Movement-Driven Nanogenerator. *Nano Lett.* **2009**, *9*, 1201–1205.
7. Xu, S.; Qin, Y.; Xu, C.; Wei, Y.; Yang, R.; Wang, Z. L. Self-Powered Nanowire Devices. *Nat. Nanotechnol.* **2010**, *5*, 366–373.
8. Klimiec, E.; Zaraska, W.; Zaraska, K.; Gasiorski, K. P.; Sadowski, T.; Pajda, M. Piezoelectric Polymer Films as Power Converters for Human Powered Electronics. *Microelectron. Reliab.* **2008**, *48*, 897–901.
9. Heller, A. Miniature Biofuel Cells. *Phys. Chem. Chem. Phys.* **2004**, *6*, 209–216.
10. Mano, N.; Mao, F.; Heller, A. Characteristics of a Miniature Compartment-less Glucose−O_2 Biofuel Cell and Its Operation in a Living Plant. *J. Am. Chem. Soc.* **2003**, *125*, 6588–6594.
11. Yan, Y.; Zheng, W.; Su, L.; Mao, L. Carbon-Nanotube-Based Glucose/O_2 Biofuel Cells. *Adv. Mater.* **2006**, *18*, 2639–2643.
12. Chang, C.; Tran, V. H.; Wang, J.; Fuh, Y.; Lin, L. Direct-Write Piezoelectric Polymeric Nanogenerator with High Energy Conversion Efficiency. *Nano Lett.* **2010**, *10*, 726−731.
13. Li, D.; Wang, Y.; Xia, Y. Electrospinning of Polymeric and Ceramic Nanofibers as Uniaxially Aligned Arrays. *Nano Lett.* **2003**, *3*, 1167–1171.
14. Zheng, J.; He, A.; Li, J.; Han, C. C. Polymorphism Control of Poly(vinylidene fluoride) through Electrospinning. *Macromol. Rapid Commun.* **2007**, *28*, 2159–2162.
15. Sirohi, J.; Chopra, I. Fundamental Understanding of Piezoelectric Strain Sensors. *J. Intell. Mater. Syst. Struct.* **2000**, *11*, 246–257.
16. Kenney, J. M.; Roth, S. C. Room Temperature Poling of Poly(Vinylidene Fluoride) with Deposited Metal Electrodes. *J. Res. Natl. Bur. Stand.* **1979**, *84*, 447–453.
17. Bauer, S. Poled Polymers for Sensors and Photonic Application. *J. Appl. Phys.* **1996**, *80*, 5531–5558.
18. Guiseppi-Elie, A.; Lei, C.; Baughman, R. H. Direct Electron Transfer of Glucose Oxidase on Carbon Nanotubes. *Nanotechnology* **2002**, *13*, 559–564.
19. Luong, J. H. T.; Hrapovic, S.; Wang, D.; Bensebaa, F.; Simard, B. Solubilization of Multiwall Carbon Nanotubes by 3-Aminopropyltriethoxysilane Towards the Fabrication of Electrochemical Biosensors with Promoted Electron Transfer. *Electroanalysis* **2004**, *16*, 132–139.
20. Cai, C.; Chen, J. Direct Electron Transfer of Glucose Oxidase Promoted by Carbon Nanotubes. *Anal. Biochem.* **2004**, *332*, 75−83.
21. Lumley-Woodyear, T.; Rocca, P.; Lindsay, J.; Dror, Y.; Freeman, A.; Heller, A. Polyacrylamide-Based Redox Polymer for Connecting Redox Centers of Enzymes to Electrodes. *Anal. Chem.* **1996**, *67*, 1332–1338.
22. Barton, S. C.; Kim, H.; Binyamin, G.; Zhang, Y.; Heller, A. The "Wired" Laccase Cathode: High Current Density Electroreduction of O_2 to Water at +0.7 V (NHE) at pH 5. *J. Am. Chem. Soc.* **2001**, *123*, 5802–5803.
23. Mano, N.; Mao, F.; Heller, A. A Miniature Biofuel Cell Operation in A Physiological Buffer. *J. Am. Chem. Soc.* **2002**, *124*, 12962–12963.
24. Xu, C.; Wang, X.; Wang, Z. L. Nanowire Structured Hybrid Cell for Concurrently Scavenging Solar and Mechanical Energies. *J. Am. Chem. Soc.* **2009**, *131*, 5866–5872.